PAPER

Maleic anhydride derivatives as catalysts for *N*-oxidation of pyridine using hydrogen peroxide†

Ghellyn Gajeles, [ID] ‡* Kyung-Koo Lee [ID] and Sang Hee Lee [ID]

Maleic anhydride derivatives were evaluated as catalysts in *N*-oxidation of various pyridine substrates using hydrogen peroxide (H_2O_2). Depending on the electronic properties of the pyridine substrates, pyridines with electron-donating groups reacted well with 2,3-dimethylmaleic anhydride (**DMMA**). In contrast, 1-cyclohexene-1, 2-dicarboxylic anhydride (**CHMA**) was most effective for electron-deficient pyridines. The different performance of these two anhydrides is attributed to the diacid–anhydride equilibrium, which is crucial for regenerating the peracid oxidant through an anhydride intermediate in the catalytic cycle. This approach using a catalytic amount of anhydride with H_2O_2 has the potential to replace stoichiometric amounts of percarboxylic acid as an oxidant for a broader range of organic substrates.

1   Introduction

Due to its safe, cheap, clean, and environmentally friendly properties, hydrogen peroxide (H_2O_2) is a preferred oxidant, producing only molecular oxygen and water as by-products.[1] Although it is a powerful oxidant with high potential, H_2O_2's high activation barriers make it less effective under mild conditions.[2–5] To address this limitation and enhance its activity, H_2O_2 requires activation by an additional reagent that functions as the terminal oxidant.[6,7] This has led to the development of numerous catalytic systems utilizing H_2O_2, with a significant focus on metal-catalyzed oxidations.[8–13] Unfortunately, the use of metal catalysts can introduce safety concerns, particularly when producing high-purity pharmaceutical compounds. Metal-free H_2O_2 oxidation procedures have emerged as a promising solution to address this challenge.[14–17]

Organocatalytic oxidations with H_2O_2 have recently gained attraction as a powerful and convenient method for synthesizing diverse molecules due to their mild reaction conditions and reduced toxicity.[18–20] Various organic catalysts have been explored as mediators for H_2O_2-based oxidations, including aldehydes,[21] hydroxamic acids,[22] flavins,[23] alloxan,[24] heteroarenium salts,[25–27] benzoxathiazines,[28,29] and aryl trifluoromethyl ketones.[30–33] Some organocatalysts have been shown to enable asymmetric transformations such as *N*-oxidation,[34,35] epoxidation,[36] and hydroxylation.[37]

The percarboxylic acids are significantly stronger oxidants compared to H_2O_2. However, due to their instability, percarboxylic acids are typically generated directly within the reaction mixture (*in situ*). Even though various anhydrides have been successfully employed as mediators in H_2O_2 oxidation reactions, unfortunately, mostly stoichiometric amounts of anhydride were used.[38–43]

Our previous work demonstrated anhydride-containing polymers, featuring repeating succinic anhydride units in the backbone, as effective catalysts for *N*-oxidation of pyridines using H_2O_2.[44] These anhydride-derived peracids undergo *N*-oxidation, after which the resulting dicarboxylic acid is converted back to the original anhydride. This regeneration step is essential for a sustained catalytic cycle, allowing the catalyst to be reused for further oxidation reactions. Maleic anhydride is expected to be more readily regenerated from its corresponding diacid compared to succinic anhydride.[45] Furthermore, the stronger acidity of maleic acid ($pK_a = 1.93$) compared to succinic acid ($pK_a = 4.21$) suggests that maleic anhydride has the potential to form a stronger peracid oxidant with H_2O_2. Motivated by this anticipated faster regeneration and stronger peracid formation, this study will investigate maleic anhydride derivatives as replacements for succinic anhydride in our previously reported catalyst system for *N*-oxidation of pyridine derivatives with H_2O_2.

2   Experimental

2.1   Materials and instruments

Pyridine derivatives and anhydride derivatives were purchased from Sigma-Aldrich and TCI and used without further purification. Column chromatography was performed using silica gel (230–400 mesh). Hydrogen peroxide (H_2O_2, 34.5 wt%) was purchased from Samchun chemicals, Korea, and used after titration with $KMnO_4$.

Department of Chemistry, Kunsan National University, Gunsan 573-701, Republic of Korea. E-mail: leesh@kunsan.ac.kr

† Electronic supplementary information (ESI) available. See DOI: https://doi.org/10.1039/d4ra05962j

‡ Physical Science Department, West Visayas State University, Luna St., La Paz, Iloilo City, 5000 Iloilo, Philippines is the authors present address.

^{1}H NMR and ^{13}C NMR spectra were obtained on a 500 MHz Agilent (VARIAN) VNMRS spectrometer. GC experiments were performed on a Shimadzu GC-2010 Gas Chromatograph equipped with a DB-5 column (30 m, 0.25 mm i.d., 0.25 μm film thickness). N$_2$ was used as the carrier gas at a flow rate of 0.87 ml min^{-1}. The oven temperature program began at 60 °C and increased linearly to 300 °C at 15 °C min^{-1}, followed by a hold at 300 °C for 4 min. The total analysis time for each sample was 20 min. The injector and detector (FID) temperatures were both set to 300 °C.

2.2 N-Oxidation reaction

In screening for anhydride catalysts at room temperature, the reaction was conducted with 1 mmol of substrate, 0.1 equivalent of anhydride catalyst, and 1.2 equivalents of 30% H$_2$O$_2$ under vigorous stirring for 24 hours. The reaction mixture is homogeneous in acetonitrile (CH$_3$CN). However, without acetonitrile, all reactions became two-phase systems (water/substrate layer) with the anhydride catalyst being soluble in the substrate layer. The conversion yield was analyzed by GC after the reaction mixture is diluted by acetonitrile.

To achieve complete N-oxidation, the reaction was conducted with 0.05 equivalent of catalyst, 2.0 equivalents of 30% H$_2$O$_2$, and vigorous stirring at 80 °C until complete conversion was observed by TLC. The reaction mixture was extracted with dichloromethane and then chromatographed (SiO$_2$, dichloromethane/methanol = 20/1) to isolate and analyze the N-oxide product by ^{1}H NMR and ^{13}C NMR spectroscopy for structure determination. To estimate the conversion percentage, 0.1 ml of the reaction in DMSO-d$_6$ mixture was analyzed by ^{1}H NMR spectroscopy. The relative integrals of the peaks corresponding to the starting material and the product were used to calculate the conversion percentage.

2.3 ^{13}C NMR analysis of composition in anhydride-H$_2$O$_2$ solution

For analysis of the composition of **CHMA** and **DMMA** in perhydrolysis reaction media, ^{13}C NMR sample solution was prepared by dissolving 1.0 mmol of anhydride and 2.0 mmol of H$_2$O$_2$ (0.20 ml, 30% wt), in 1.0 ml of CD$_3$CN. Similarly, for analysis of the composition of **CHMA** in N-oxidation media, the NMR sample solution was prepared by dissolving 2.0 mmol of pyridine derivative, 1.0 mmol of **CHMA**, and 2.0 mmol of H$_2$O$_2$ (0.20 ml, 30% wt) in 1 ml of CD$_3$CN. The ^{13}C NMR spectra were acquired at intervals throughout the incubation at room temperature.

3 Results and discussion

3.1 Screening of anhydride catalysts

2-Chloropyridine (**CP**) and quinoline were chosen as model substrates due to their differing nitrogen atom nucleophilicity in N-oxidation reaction. Readily available maleic anhydride derivatives were evaluated for their catalytic activity in N-oxidation using H$_2$O$_2$ (Fig. 1). The reaction was conducted using 1 mmol of substrate, 0.1 equivalent of anhydride catalyst, 1.2
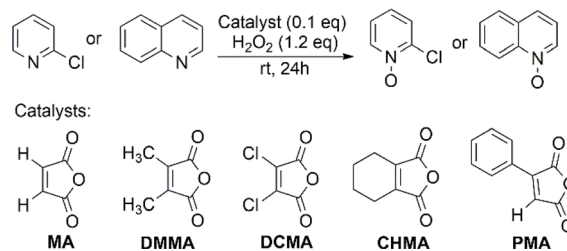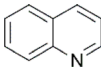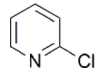

Fig. 1 Model reaction for screening the catalytic activity of anhydride catalysts.

equivalent of H$_2$O$_2$ (30%) at room temperature for 24 hours. The reaction mixture is homogeneous in acetonitrile (CH$_3$CN), but in its absence, all reactions became two-phase systems (water/substrate layer) with the anhydride catalyst being soluble in the substrate layer.

The results are shown in Table 1. As expected for electron-rich substrates being more reactive in N-oxidation, 2,3-dimethyl maleic anhydride (**DMMA**) yielded a high N-oxide conversion (70%) for quinoline, especially in two-phase reactions, but showed no catalytic activity for the electron-deficient pyridine substrate **CP**. The exceptionally high activity of **DMMA** toward quinoline in two-phase reactions likely relates to the high partition coefficient of H$_2$O$_2$ favoring quinoline over water.[46] This creates a localized environment enriched in H$_2$O$_2$, minimizing the amount of water surrounding the reactants, which is beneficial for the reaction.

2,3-Dichloromaleic acid, derived from dichloromaleic anhydride (**DCMA**) is a strong acid with pK_{a_1} < 1.72 and pK_{a_2} < 3.86 (compare to pK_{a_1} = 1.72 and pK_{a_2} = 3.86 for chloromaleic acid) due to the electron-withdrawing effect of the two chlorine atoms.[47] This suggests its potential effectiveness for less reactive substrates like **CP** and agrees well with the results (25%). However, intriguingly, **DCMA** showed no activity towards quinoline, which is a more readily oxidized substrate. This lack of activity for the more reactive quinoline can be attributed to the high basicity of quinoline (pK_a = 4.93).[48] Quinoline can deprotonate both of the carboxylic acid groups on the diacid form of **DCMA**, leading to salt formation. This disrupts the anhydride-diacid equilibrium, preventing regeneration of the

Table 1 Reactivity of anhydride catalysts in N-oxidation of pyridine derivatives^a

| Substrate | Solvent | Conversion^b (%) | | | | |
		MA	**DMMA**	**DCMA**	**CHMA**	**PMA**
(quinoline)	Water	13	**70**	1	**24**	17
	CH$_3$CN	8	8	0	**24**	12
(2-chloropyridine)	Water	6	0.3	14	**29**	10
	CH$_3$CN	0	0	25	**32**	9

^{a} Reaction condition: substrate, 1 mmol; anhydride, 0.1 eq.; H$_2$O$_2$, 1.2 eq.; 24 h at room temperature. ^{b} Conversion (%) determined by gas chromatography.

active anhydride and halting the *N*-oxidation catalytic cycle (Fig. 2). Conversely, due to its much lower basicity ($pK_a = 0.54$) compared to quinoline, **CP** cannot deprotonate **DCMA**. This allows the diacid to readily convert back to the active anhydride species, maintaining the *N*-oxidation catalytic cycle. In contrast to the substrate-dependent activity observed with **DMMA** and **DCMA**, **CHMA** is effective for both **CP** and quinoline substrates (24–32%), regardless of whether CH_3CN solvent is used. This suggests that **CHMA** may be less sensitive to the electronic properties of the substrate compared to other anhydride catalysts. To elucidate the contrasting catalytic activities of **DMMA** and **CHMA** in *N*-oxidation reactions, a mechanistic investigation was undertaken.

3.2 Mechanistic investigation of DMMA and CHMA

Peracid formation, a crucial step in *N*-oxidation where an organic acid gains oxygen from H_2O_2, is likely similar to succinic acid's amidation, where anhydride formation is the rate-limiting step.[49] We propose that peracid formation from a diacid also proceeds *via* an anhydride intermediate (Fig. 3). Therefore, the rate of *N*-oxidation likely depends on the concentration of the active anhydride species, which is related to the equilibrium constant (K_{eq}) between the diacid and the anhydride. In this context, a study by Eberson on cyclic anhydrides investigating their equilibrium behavior in aqueous solution is relevant.[50] This study found that the equilibrium constants (K_{eq}) for the hydrolysis of **DMMA** and **CHMA** were 5.3 and <0.1, respectively. These significant differences in K_{eq} values for **DMMA** and **CHMA** in aqueous H_2O_2 solution likely explain their contrasting catalytic performance in *N*-oxidation. The lower K_{eq} value for **CHMA** indicates a smaller equilibrium concentration of the active anhydride species (precursor to the peracid) compared to **DMMA**. The difference in their K_{eq} values can be attributed to their structural differences. As shown in Fig. 4, the methyl group in **DMMA** is more flexible than the methylene group in the cyclohexene ring of **CHMA**. This increased flexibility may contribute to greater steric hindrance during the hydrolysis of the anhydride, due to the bulkier nature of the methyl group. Additionally, the flexibility of the **DMMA** methyl group could facilitate the alignment of two carboxyl groups for anhydride formation.

To understand the distribution of species in the **CHMA**-H_2O_2 reaction mixture, which is crucial for its catalytic activity, we
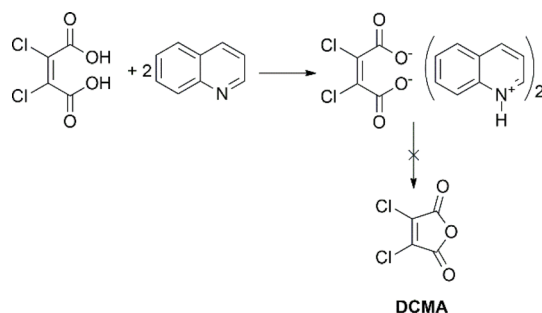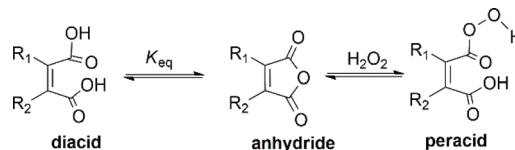

Fig. 3 Formation of peracid from diacid *via* anhydride intermediate.

investigated the molar fractions of anhydride, diacid, and peracid present at equilibrium. While the ^{1}H NMR spectrum of the mixture cannot differentiate the protons of the anhydride, peracid, and diacid, the ^{13}C NMR spectrum (Fig. 5) fortunately allows for clear distinction of the aliphatic carbons 'a' and 'b' of each species. For similarly connected molecules such as diastereomers, ^{13}C NMR integration with standard broadband decoupling (BBD) closely matches peak areas obtained from ^{1}H NMR, within 3.4%.[51] This study proposes that quantification using ^{13}C NMR integration values of carbon "a" and "b" in **CHMA** derivatives can be correlated well with the actual amounts determined by ^{1}H NMR data. For quantification, we preferentially chose carbon 'b' due to its distance from the carbonyl group, which minimizes interference with the integration value caused by relaxation effects.

A homogeneous solution containing **CHMA** (1.0 mmol) and H_2O_2 (2.0 mmol) in deuterated acetonitrile (CD_3CN) (1 ml) was analyzed using ^{13}C NMR spectroscopy. ^{13}C NMR analysis of the reaction mixture after incubation for 1 hour at room temperature revealed the formation of approximately 38% peracid and 6% diacid, with the remaining 56% being the starting **CHMA** (Fig. 6). After 48 hours, the reaction reaches equilibrium, with the relative amounts of anhydride (31%), diacid (49%), and peracid (20%) indicating a dynamic interplay between these species. In the initial stages, **CHMA** likely undergoes perhydrolysis with H_2O_2 rather than hydrolysis due to its higher nucleophilicity compared to water. Interestingly, at equilibrium, the diacid concentration is higher than the peracid concentration. This suggests a faster conversion of peracid back to anhydride compared to the conversion rate of diacid back to anhydride. Maintaining the high presence of anhydride at equilibrium (around 31%) likely stems from its continuous regeneration *via* the equilibrium with the diacid and peracid forms. This continuous regeneration cycle is proposed to be essential for **CHMA**'s effectiveness as an *N*-oxidation catalyst. It is noteworthy that requiring more than 24 hours to reach complete equilibrium indicates a very slow conversion of diacid to anhydride. Therefore, to achieve fast oxidation, the reaction temperature should be elevated to accelerate the anhydride regeneration rate, independent of the substrate's reactivity.
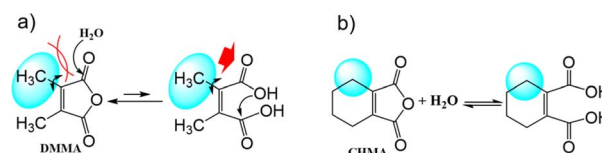

Fig. 2 Deactivation of DCMA through salt formation.

Fig. 4 Structural differences of (a) DMMA, and (b) CHMA.
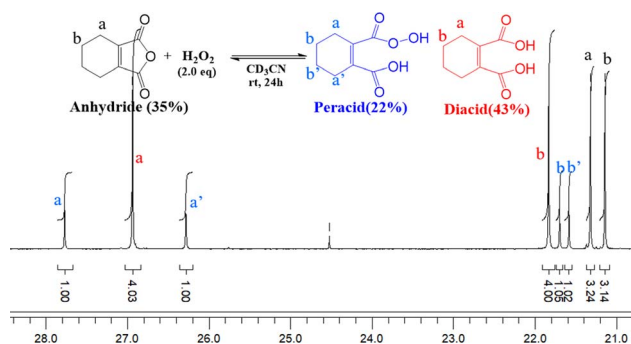
Fig. 5 ^{13}C NMR spectrum of **CHMA** in H$_2$O$_2$ and CD$_3$CN after 24 h at room temperature.
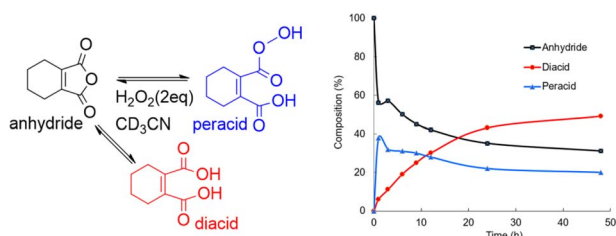
Fig. 6 Composition change in the perhydrolysis of **CHMA** in CD$_3$CN–H$_2$O$_2$ at room temperature.

Perhydrolysis of **DMMA** yielded only 1.2% of diacid and no detectable peracid according to ^{13}C NMR analysis (Fig. 7, and ESI, SI-3C†). This suggests a strong preference for the anhydride form in equilibrium with H$_2$O$_2$. The equilibrium constant (K_{eq}) of **DMMA** in a solution of H$_2$O$_2$ (2.0 eq., 30%) and CD$_3$CN is 84, significantly higher compare to **DMMA**'s value in aqueous solution (K_{eq} = 5.3).[50] In addition to the absence of peracid accumulation, the fast regeneration of anhydride can be seen in Fig. 7. The rapid anhydride regeneration favors the reaction with highly reactive substrates such as quinoline because the resulting peracid can react with substrate before it converts back to anhydride. Conversely, for oxidizing less reactive substrate like **CP**, some amount of peracid accumulation, as seen in **CHMA**, is likely crucial.

To understand the mechanistic differences in **CHMA**'s oxidation activity towards quinoline and **CP**, the reaction mixtures were monitored by ^{13}C NMR spectroscopy at room temperature (Fig. 8). The analysis revealed a clear trend,

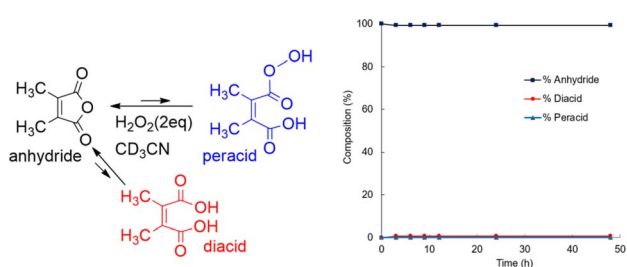consistent with quinoline being significantly more reactive than **CP**. This is evident from the higher N-oxide yield for quinoline (76%) compared to **CP** (17%). Furthermore, the ^{13}C NMR spectra showed a gradual depletion of the anhydride intermediate in the **CP** reaction, while it was rapidly consumed in the quinoline reaction. Additionally, the peracid intermediate observed during **CP** oxidation is not detectable in quinoline oxidation. This suggests that the highly reactive quinoline rapidly consumes the peracid oxidant, preventing its significant accumulation. Based on these observations, the rate-limiting step for quinoline oxidation is likely the formation of anhydride (k_3), while for **CP**, it's the N-oxidation step (k_2) (Fig. 9).

3.3 Scope of application of DMMA and CHMA

DMMA and **CHMA** are effective catalysts for the N-oxidation of reactive substrates such as quinoline, even at room temperature, as demonstrated in Table 1 and Fig. 8. However, for less reactive substrates, the reaction temperature must be increased to accelerate the reaction rate. To compare the catalytic performance of **DMMA** and **CHMA** in the N-oxidation of various pyridine derivatives, reactions were conducted at 80 °C. The required reaction time for complete N-oxidation and the conversion yield after a 14 hours reaction (for slow reactions) are summarized in Table 2.

Both **DMMA** and **CHMA** effectively catalyze the N-oxidation of reactive substrates (entries 1–4). Steric hindrance around the nitrogen atom, as observed in entry 3, slows down the reaction rate. For electron-deficient substrates, **CHMA** outperforms **DMMA**. **CHMA** is generally effective for both electron-rich and electron-poor substrates (entries 1–8), except for highly deactivated compounds (entries 9 and 10). Interestingly, 2-picolinic acid (entry 6) exhibits exceptionally high reactivity compared to entries 7 and 8, despite being an electron-poor substrate. This enhanced reactivity is likely attributed to hydrogen bonding between the *ortho*-carboxyl group of 2-picolinic acid and the peracid. The resulting proximity of the peracid to the nitrogen atom, facilitated by this interaction, promotes the reaction. Based on these results, it is postulated that **DMMA** is superior to **CHMA** for reactive substrates, while **CHMA** is a better choice for less reactive electron-deficient substrates. The catalytic performance of **DMMA** and **CHMA** is influenced by both substrate nucleophilicity and steric hindrance.
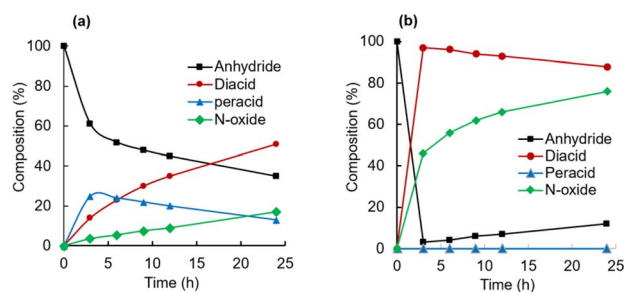

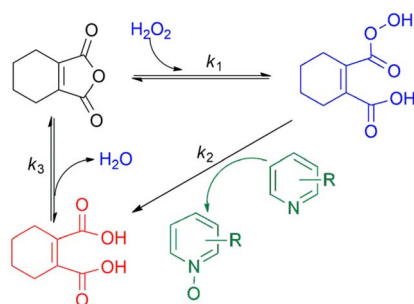**Fig. 7** Composition change in the perhydrolysis of **DMMA** in CD$_3$CN–H$_2$O$_2$ at room temperature.

Fig. 8 Composition changes during N-oxidation of **CP** (a) and quinoline (b) by **CHMA** (1.0 eq.) and H$_2$O$_2$ (2.0 eq.) in CD$_3$CN at room temperature.

Fig. 9   Catalytic cycle of CHMA in N-oxidation.

Table 2   N-Oxidation using DMMA and CHMA catalysts[a]

Entry	Substrate	Conversion[b] (%) (reaction time, h)	
		DMMA	CHMA
1		100 (3)	100 (5)
2		100 (5)	100 (12)
3		97[c] (14)	88 (14)
4		100 (3)	98[c] (3)
5		37 (14)	96[c] (5)
6		98 (14)	100 (2)
7		80 (14)	100 (7)
8		13 (14)	92 (14)
9		0 (14)	4 (14)
10		0 (14)	0 (14)

[a] Reaction condition: substrate (1 mmol); anhydride (0.05 eq.); H_2O_2 (2.0 eq., 30%) at 80 °C. [b] Conversions (%) determined by ^{1}H NMR of the crude reaction mixtures. [c] Isolated yield (%).

4   Conclusions

Among the maleic anhydride derivatives, **DMMA** and **CHMA** exhibit excellent catalytic activity in pyridine N-oxidation using H_2O_2. The rapid regeneration of the anhydride from diacid facilitates the catalytic cycle, as anhydride is readily available for conversion to the peracid. **DMMA** shows good catalytic activity

for the N-oxidation of reactive substrates like pyridine, 2-methyl pyridine, and quinoline; whereas **CHMA** is efficient in oxidizing deactivated pyridine substrates such as **CP**.

This catalytic system, employing a catalytic amount of anhydride with H_2O_2 as the oxidant, offers a promising alternative to stoichiometric percarboxylic acid oxidants such as m-chloroperoxybenzoic acid (mCPBA). This advantage extends to a broad range of organic substrate oxidations, including olefin epoxidation, sulfide oxidation, Baeyer–Villiger oxidation, etc. A mechanistic study of the vastly different catalytic performances of **DMMA** and **CHMA** offered valuable insights for selecting suitable anhydride catalysts in other oxidation reactions.

To achieve optimal catalytic performance and promote green chemistry principles in H_2O_2 oxidation, further exploration of two promising avenues is recommended: structural modification of anhydride molecules and development of recyclable maleic anhydride catalysts through immobilization.

Data availability

The data supporting this article have been included as part of the ESI.†

Conflicts of interest

There are no conflicts to declare.

Acknowledgements

References

1 H. Targhan, P. Evans and K. Bahrami, *J. Ind. Eng. Chem.*, 2021, **104**, 295–332.
2 J. M. Campos-Martin, G. Blanco-Brieva and J. L. Fierro, *Angew. Chem., Int. Ed.*, 2006, **45**, 6962–6984.
3 J. Kraïem, D. Ghedira and T. Ollevier, *Green Chem.*, 2016, **18**, 4859–4864.
4 R. Noyori, M. Aoki and K. Sato, *Chem. Commun.*, 2003, 1977–1986, DOI: **10.1039/b303160h**.
5 W. R. Sanderson, *Pure Appl. Chem.*, 2000, **72**, 1289–1304.
6 M. V. Doble, A. C. Ward, P. J. Deuss, A. G. Jarvis and P. C. Kamer, *Bioorg. Med. Chem.*, 2014, **22**, 5657–5677.
7 B. Martin, J. Sedelmeier, A. Bouisseau, P. Fernandez-Rodriguez, J. Haber, F. Kleinbeck, S. Kamptmann, F. Susanne, P. Hoehn, M. Lanz, L. Pellegatti, F. Venturoni, J. Robertson, M. C. Willis and B. Schenkel, *Green Chem.*, 2017, **19**, 1439–1448.
8 M. Alem, S. Kazemi, A. Teimouri and H. Salavati, *Asian J. Green Chem.*, 2019, **3**, 366–381.

9 Y. Ding, W. Zhao, W. Song, Z. Zhang and B. Ma, *Green Chem.*, 2011, **13**(6), 1486–1489.

10 Y. Kon, *J. Jpn. Pet. Inst.*, 2017, **60**, 159–169.

11 N. Mizuno and K. Kamata, *Coord. Chem. Rev.*, 2011, **255**, 2358–2370.

12 F. Sadri, A. Ramazani, A. Massoudi, M. Khoobi, R. Tarasi, A. Shafiee, V. Azizkhani, L. Dolatyari and S. W. Joo, *Green Chem. Lett. Rev.*, 2014, **7**, 257–264.

13 W. Xie, Y. Zheng, S. Zhao, J. Yang, Y. Liu and P. Wu, *Catal. Today*, 2010, **157**, 114–118.

14 A. Rostami, Y. Navasi, D. Moradi and A. Ghorbani-Choghamarani, *Catal. Commun.*, 2014, **43**, 16–20.

15 S. Rostamnia, B. Gholipour and H. Golchin Hosseini, *Process Saf. Environ. Prot.*, 2016, **100**, 74–79.

16 F. Secci, A. Frongia and P. P. Piras, *Tetrahedron Lett.*, 2014, **55**, 603–605.

17 Q. Wei, H. Fan, F. Qin, Q. Ma and W. Shen, *Carbon*, 2018, **133**, 6–13.

18 E. T. Poursaitidis, P. L. Gkizis, I. Triandafillidi and C. G. Kokotos, *Chem. Sci.*, 2024, **15**, 1177–1203.

19 A. Russo, C. De Fusco and A. Lattanzi, *ChemCatChem*, 2012, **4**, 901–916.

20 K. A. Stingl and S. B. Tsogoeva, *Tetrahedron: Asymmetry*, 2010, **21**, 1055–1074.

21 I. Triandafillidi, M. G. Kokotou, D. Lotter, C. Sparr and C. G. Kokotos, *Chem. Sci.*, 2021, **12**, 10191–10196.

22 E. T. Poursaitidis, F. Trigka, C. Mantzourani, M. G. Kokotou, I. Triandafillidi and C. G. Kokotos, *Eur. J. Org Chem.*, 2024, **27**, e202400082.

23 K. Bergstad and J.-E. Bäckvall, *J. Org. Chem.*, 1998, **63**, 6650–6655.

24 S. Zhang, G. Li, L. Li, X. Deng, G. Zhao, X. Cui and Z. Tang, *ACS Catal.*, 2019, **10**, 245–252.

25 P. Ménová, F. Kafka, H. Dvořáková, S. Gunnoo, M. Šanda and R. Cibulka, *Adv. Synth. Catal.*, 2011, **353**, 865–870.

26 J. Sturala, S. Bohacova, J. Chudoba, R. Metelkova and R. Cibulka, *J. Org. Chem.*, 2015, **80**, 2676–2699.

27 D. Wang, W. G. Shuler, C. J. Pierce and M. K. Hilinski, *Org. Lett.*, 2016, **18**, 3826–3829.

28 B. H. Brodsky and J. Du Bois, *J. Am. Chem. Soc.*, 2005, **127**, 15391–15393.

29 N. D. Litvinas, B. H. Brodsky and J. Du Bois, *Angew. Chem., Int. Ed.*, 2009, **48**, 4513–4516.

30 D. Limnios and C. G. Kokotos, *J. Org. Chem.*, 2014, **79**, 4270–4276.

31 D. Limnios and C. G. Kokotos, *Chemistry*, 2014, **20**, 559–563.

32 C. J. Pierce and M. K. Hilinski, *Org. Lett.*, 2014, **16**, 6504–6507.

33 I. Triandafillidi, D. I. Tzaras and C. G. Kokotos, *ChemCatChem*, 2018, **10**, 2521–2535.

34 S. Y. Hsieh, Y. Tang, S. Crotti, E. A. Stone and S. J. Miller, *J. Am. Chem. Soc.*, 2019, **141**, 18624–18629.

35 S. E. Huth, E. A. Stone, S. Crotti and S. J. Miller, *J. Org. Chem.*, 2023, **88**, 12857–12862.

36 M. Marigo, J. Franzen, T. B. Poulsen, W. Zhuang and K. A. Jorgensen, *J. Am. Chem. Soc.*, 2005, **127**, 6964–6965.

37 M. Cai, K. Xu, Y. Li, Z. Nie, L. Zhang and S. Luo, *J. Am. Chem. Soc.*, 2021, **143**, 1078–1087.

38 K. Bahrami, M. Khodaei and A. Karimi, *Synthesis*, 2008, **2008**, 1682–1684.

39 S. Caron, N. M. Do and J. E. Sieser, *Tetrahedron Lett.*, 2000, **41**, 2299–2302.

40 B. Karami, M. Montazerozohori and M. H. Habibi, *Molecules*, 2005, **10**, 1358–1363.

41 I. Likhotvorik, M. Lutz and M. Wenzler, *Synthesis*, 2018, **50**, 2231–2234.

42 J. Liu, X.-Y. Wei, Y.-G. Wang, D.-D. Zhang, T.-M. Wang, J.-H. Lv, J. Gui, M. Qu and Z.-M. Zong, *Fuel*, 2015, **142**, 268–273.

43 P. Pietikäinen, *J. Mol. Catal. A: Chem.*, 2001, **165**, 73–79.

44 G. Gajeles, S. M. Kim, J.-C. Yoo, K.-K. Lee and S. H. Lee, *RSC Adv.*, 2020, **10**, 9165–9171.

45 L. Eberson and H. Welinder, *J. Am. Chem. Soc.*, 1971, **93**, 5821–5826.

46 J. H. Walton and H. A. Lewis, *J. Am. Chem. Soc.*, 2002, **38**, 633–638.

47 R. Williams, *Bordwell pKa Table*, **https://organicchemistrydata.org/hansreich/resources/pka/pka_data/pka-compilation-williams.pdf**, (accessed August 10, 2024).

48 M. Lõkov, S. Tshepelevitsh, A. Heering, P. G. Plieger, R. Vianello and I. Leito, *Eur. J. Org Chem.*, 2017, **2017**, 4475–4489.

49 T. Higuchi, L. Eberson and J. D. McRae, *J. Am. Chem. Soc.*, 1967, **89**, 3001–3004.

50 L. Eberson, J. Sundman, I. Toplin, A. Melera and L. Nilsson, *Acta Chem. Scand.*, 1964, **18**, 1276–1282.

51 D. A. Otte, D. E. Borchmann, C. Lin, M. Weck and K. A. Woerpel, *Org. Lett.*, 2014, **16**, 1566–1569.